Atmospheric and Climate Sciences, 2016, 6, 367-374
Published Online July 2016 in SciRes. http://www.scirp.org/journal/acs
http://dx.doi.org/10.4236/acs.2016.63030

Current Networks of Long Proxies for Building Reconstruction Models of the Atlantic Multidecadal Oscillation

Markus Lindholm[1], Risto Jalkanen[1], Maxim G. Ogurtsov[2]

[1]Luke, Rovaniemi Research Unit, Rovaniemi, Finland
[2]A.F. Ioffe Physico-Technical Institute, St. Petersburg, Russia
Email: hmw.lindholm@gmail.com, maxim.ogurtsov@mail.ioffe.ru

Received 10 December 2015; accepted 20 May 2016; published 23 May 2016

Abstract

Currently available proxies were studied as networks for building reconstruction models of the Atlantic Multidecadal Oscillation (AMO). Only proxies that would double the current record length (backwards in time from AD 1564) were included. We present two proxy networks and corresponding reconstruction (transfer) models, one for tree-growth based proxies only and another for multiproxies. Both of them show a useful match in timing as well as amplitude with the AMO. These model structures demonstrated reasonable model performance (overall r^2 = 0.45 - 0.36). The time stability of proxy-AMO relationships was also validated. The new models produced acceptable results in cross-calibration-verification (reduction of error and coefficient of efficiency statistics in 1856-1921 and 1922-1990 vary between 0.41 and 0.21). The spatial distribution of these data series indicate that proxies respond to an AMO-like climatic oscillation over much of the Northern Hemisphere.

Keywords

Proxies, Atlantic Multidecadal Oscillation, Tree Growth, Climate Change, Transfer Models

1. Introduction

North Atlantic sea-surface temperatures (SSTs) are known to vary prominently on multidecadal timescales. These variations are dominated by the alternation between warm and cold SST anomalies on an oscillating timescale of 60 - 80 years. The AMO has been identified in the instrumental record as a coherent, basin-wide pattern of oscillatory changes in SST [1]-[3]. On Hemispheric scale, it also seems likely that an atmospheric

How to cite this paper: Lindholm, M., Jalkanen, R. and Ogurtsov, M.G. (2016) Current Networks of Long Proxies for Building Reconstruction Models of the Atlantic Multidecadal Oscillation. *Atmospheric and Climate Sciences*, **6**, 367-374.
http://dx.doi.org/10.4236/acs.2016.63030

bridge conveys the influence of the Atlantic Ocean to the Pacific modulating the El Niño-Southern Oscillation (ENSO) and Pacific Decadal Oscillation (PDO) [4] [5].

The forcing mechanism pacing the AMO remains subject to considerable debate. On one hand, the AMO is thought to be driven by internal ocean variability and is related to multidecadal fluctuations in the Atlantic Meridional Overturning Circulation [1] [6] [7]. On the other hand, a combination of external forcing due to solar variability, e.g. volcanic eruptions, may have determined the pace and phasing of the AMO [8] [9]. A major shortcoming in assessing the true nature of the AMO as well as the underlying forcing mechanisms has been the shortness of the instrumental record (from 1856 to the present). Proxy reconstructions are irreplaceable tools in overcoming this problem.

We focused here on building networks of long proxies available from open archives as well as studying their potential in modeling the AMO. The well-known reconstruction of the AMO since AD 1567 by Gray *et al.* [10] based on twelve total-ring-width records was used as an example. We now included only proxies that extended back to the 11th century and thus would double the length of the current record, 423 years from 1567 to 1990 by Gray *et al.* [10] to exceed 900 years. Limiting the analyses only to proxies that cover the entire time interval is a reasonable expectation since the number of available data is increasing and the archives of e.g. the International Tree-Ring Data Bank (ITRDB) are being actively updated. Secondly, we aimed to include not only tree-ring data but also other types of climate proxies with resolutions corresponding to those of the target (e.g. lake and sea-floor sediments as well as isotopic analyses from speleothems and ice). Because of potentially worldwide climate impacts [7], we studied an AMO signal in proxy networks from the whole Northern hemisphere and available data were thus not geographically limited to the Atlantic rim. Thirdly, we wanted to enhance current procedures of building transfer models for the AMO by applying cross-period validation for assessing the time stability of derived transfer functions.

2. Materials and Methods

Proxy data series from 0˚ - 90˚N covering the period 1100-1990 were obtained from the paleoclimate archives hosted by National Oceanic and Atmospheric Administration (NOAA) and International Tree-Ring Data Bank (ITRDB) (https://www.ncdc.noaa.gov/data-access/paleoclimatology-data/datasets). Candidate data series were screened mainly for temperature or precipitation, but they were also accepted if they were known to show some sensitivity to related climatological parameters.

If raw tree-ring measurements were available they were standardized using two methods that preserve medium and low-frequency variability: 1) the conservative negative exponential or lines of zero or negative slope (NE) [10] [11] and 2) more flexible 180-year splines (Sp180) [12]-[15]. Thus for each data set two chronologies were produced and compared. The chronologies producing better correlation with the target (see below) was selected for further analyses. If only a mean chronology (built using a known standardization method) was available it was used as such. Correspondingly the other (non-dendro) proxies were used as provided by the databanks. Common low-pass filters in AMO-studies—10-year moving averages [4] [10]—were used.

All the proxies meeting the initial requirements (minimum record length and climate sensitivity) were correlated with annual North Atlantic SST in 1856-1990 [16]. The series exceeding threshold value ($r \leq -0.25$ or ≥ 0.25) were combined to a rectangular matrix and subjected to principal components analysis (PCA), which orthogonalized the data to principal component scores (PCs). The number of PCs was then limited in a two-stage procedure. Higher-order PCs were first rejected based on the cumulative product of eigenvalues and the remaining PCs were further limited by the t-value for paired correlation, which should have an absolute value equal or greater than 1.0 [10] [17]-[19]. The PCs were then entered into linear regression to produce transfer functions and proxy models for the annual AMO.

Empirically derived equations which link proxies to changes in actual climatic time series must be validated or verified on independent data (to e.g. assess the time stability of the equations). To allow for comparison we used the same periods for calibration and verification (1922-1990, 1856-1921) as Gray *et al.* [10]. Previous AMO studies have used only one period for calibration and one for verification. Individual models were now tested further in split period calibration-verification, where each period was tested separately and independently. The two sub-periods (1856-1921, 1922-1990), used for calibration during one period and verification during the other are referred to as early calibration-late verification and late calibration-early verification (EC-LV and LC-EV, respectively). Both sub-periods should now produce positive values of reduction of error (RE) [11] [17]

[18] and coefficient of efficiency (CE) [17] [20]. RE and CE are central statistics in climate reconstruction recommended by e.g. National Research Council [20]. Their values may vary from +1 to $-\infty$. The models were also compared using correlation (r) and explained variance or coefficient of determination (r^2).

3. Results

The search for suitable proxies produced a network of 16 long series (**Table 1**). They include data of both annual and decadal resolution, which meet the initial criterion of correlation (individual proxies vs annual AMO index with r greater than |0.25|). The spread of the network and the response of these series to the AMO are shown in **Figure 1**. Nicoa Cave series (speleothem, series 3, **Table 1**, **Figure 1**) had the highest and the Finnish tree-ring (MXD) series the lowest correlation (r = 0.49 and 0.25 respectively). Three of the proxies are speleothem series and one a lake sediment series. The remaining 12 are dendrochronological data. Five of these reached higher r-values using the NE method and six with the SP180 method. One tree-ring width data set (Taimyr Peninsula, Russia, series 5, **Table 1**) was only available as regional curve standardized (RCS) chronology and was included as such.

The data set of 16 series were transformed to PCs, the number of which was first limited to 12 and then to five. These PCs (1, 2, 3, 4 and 8 with cumulative variance explained = 65%) were retained for use in building the reconstruction models. In cross-calibration-verification the model of five PCs produced positive values of RE (>0.37) and CE (>0.36) in both EC_LV and LC_EV periods (**Table 2(a)**). The early and late calibrated reconstruction models were able to explain 37% - 42% of the variance in verification period AMO with high confidence (**Table 2(a)**). Thus a full model using the entire 135-year calibration period (1856-1990) could be drawn with $r^2 = 0.45$ (**Figure 2(a)**):

a) $y = -0.0176 + 0.0474 * PC1 + 0.0119 * PC2 - 0.0359 * PC3 + 0.0257 * PC4 - 0.0197 * PC8$

The network of 16 series includes 12 tree-growth based chronologies (11 tree-ring width and one maximum-latewood density series). The above procedure was now repeated especially for these dendrochronological series.

Table 1. Name, location and type of proxy series 1 - 16 covering the 900 years period 1090-1990. Reference to principal investigator named in the data-bases or latest paper by the authors.

Proxy location	Longitude	Latitude	Proxy type	Reference
Non-dendroseries:				
1) Dongge Cave, South China	108.5	25.17	Sp	Wang *et al.* 2005
2) Socotra Island, Indian Ocean	50	12,5	Sp	Burns *et al.* 2003
3) Nicoa Cave, Nicoya, Costa Rica	−85.3	10.2	Sp	Mann *et al.* 2008
4) Lake Chichancanab, Yacatan, Mexico	−88.9	19.8	Is	Hodell *et al.* 1995, 2005
Dendroseries:				
5) Taimyr Peninsula, Russia	105	70.3 - 73	TRW	Naurzbaev *et al.* 2002
6) Torneträsk, North Sweden	19.43	68.13	TRW	Grudd *et al.* 2002
7) Laanila, North Finland	27.30	68.50	MXD	McCarroll *et al.* 2013
8) Kola Peninsula, Russia	33.15	67.41	TRW	Kononov *et al.* 2009
9) Hentii Mountains, Mongolia	107.28	48.21	TRW	Cook *et al.* 2010
10) Whirlpool Point, Alberta, Canada	−116.27	52	TRW	Sauchyn *et al.* 2011
11) North Fork Ridge, Montana, USA	−111.2	45.18	TRW	John C. King
12) Pintlers, Montana, USA	−113.22	46.01	TRW	Pederson *et al.* 2011
13) Flint Creek Range, Montana, USA	−113.09	46.17	TRW	Hughes, M.K., Woodhouse, C.A., Brown, P.M.
14) Yellow Mountain Ridge 2, Montana, USA	−111.19	45.18	TRW	Graumlich *et al.* 2002
15) Pearl Peak update, Nevada, USA	−115.32	40.14	TRW	Salzer *et al.* 2009
16) Sheep Mountain update, California, USA	−118.12	37.31	TRW	Salzer *et al.* 2009

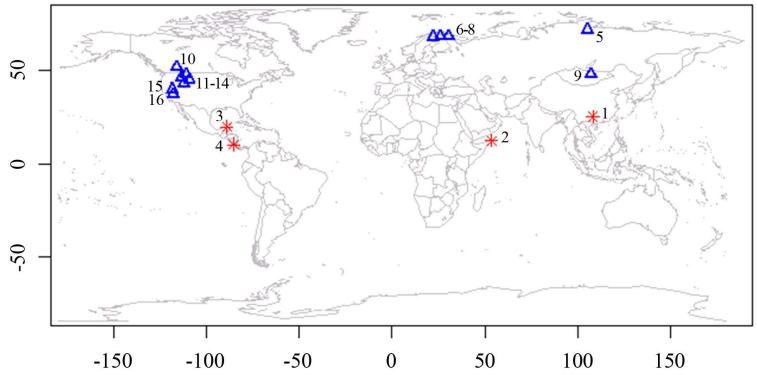

Figure 1. The network includes 16 tree-growth based (triangles) and other types of proxies (stars). Correlation with the AMO (1856-1990) in brackets: 1, Dongge Cave (−0.43); 2, Socotra Island (−0.39); 3, Nicoa Cave (0.49); 4, Lake Chichancanab (0.26); 5, Taimyr Peninsula (0.35); 6, Torneträsk (0.32); 7, Laanila (0.25); 8, Kola Peninsula (0.35); 9, Hentii Mountains (0.28); 10, Whirlpool Point (−0.25); 11, North Fork Ridge (0.25); 12, Pintlers (0.31); 13, Flint Creek Range (0.36); 14, Yellow Mountain Ridge 2 (−0.25); 15, Pearl Peak update (0.29); and 16, Sheep Mountain update (0.28).

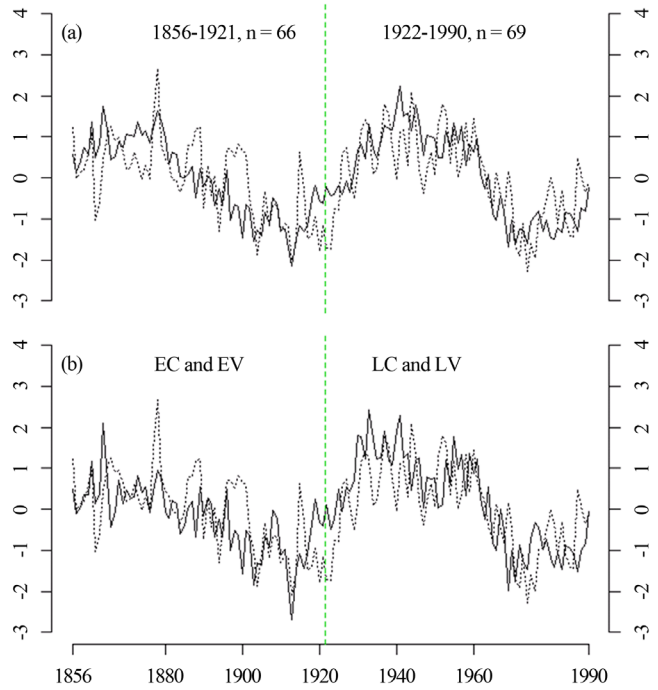

Figure 2. Actual vs. estimated values: two model structures produced using either 16 mixed proxies (a) and 12 tree-growth based proxies (b). Dotted line is the target annual AMO index. Vertical line (dash) divides the available calibration and verification periods.

Among them the series from Flint Creek Range (Montana, USA) has the highest correlation with the AMO (r = 0.36, **Figure 1**). The 12 series were now subjected to PCA and screening of PCs. Four PCs (1, 3, 5 and 8 with cumulative variance explained ~54%) now passed the screenings and were used in calibration with the AMO. In verification both EC_LV and LC_EV models had positive values of RE and CE (**Table 2(b)**). In respective verification periods these two reconstructions explain 24% - 35% of the AMO variance (**Table 2(b)**). All available data (1856-1990) were again recalibrated to build a full model with $r^2 = 0.36$ (**Figure 2(b)**):

b) $y = -0.0176 + 0.05 * PC1 - 0.0154 * PC3 + 0.0374 * PC5 - 0.0236 * PC8$

The F-statistic for final models A and B are 25.64 and 17.88 respectively–both highly significant. It is very unlikely to get F-ratios as large as these by chance alone if the slope of overall regression line were zero (H_0: no

Table 2. Calibration and verification period statistics for the two types of reconstruction models ((a) and (b)). The early calibration (1856-1921) figures are verified over the 1922-1990 period and the late calibration (1922-1990) figures are verified on the 1856-1921 data.

(a) Multiproxy from 16 series		
	Early calibration	Late calibration
Calibration r^2	0.42	0.50
Verification r^2	0.42	0.37
Significance level (p)	1.6×10^{-9}	7×10^{-8}
RE	0.41	0.37
CE	0.41	0.36
(b) Proxy from 12 dendrochronological series		
Calibrationr^2	0.35	0.42
Verification r^2	0.35	0.24
Significance level (p)	8.8×10^{-8}	2.6×10^{-5}
RE	0.31	0.21
CE	0.31	0.21

dependence of *y* on *x*).

Correlation between the annual AMO index and the reconstructions during the full (135-year) calibration period is 0.67 for model A and 0.60 for model B (**Table 3**). These results show highly significant associations since the null hypothesis can be rejected with reasonable confidence ($p \leq 2.5 \times 10^{-14}$). Using filtered data correlations rise to 0.92 and 0.87 for models A and B respectively and the relationship become even more evident (**Figure 3(a)**, **Figure 3(b)**). Despite an obvious overall resemblance, in detail model B first somewhat underestimates the AMO in late 19th century and then overestimates it in early 1900s up to around 1940 (**Figure 3(b)**). Model A performs more evenly in this respect (**Figure 3(a)**).

Additional verification was achieved by comparisons of our proxy models and the reconstruction by Gray *et al.* [10], which produced r = 0.53 for model A and r = 0.54 for model B in 1856-1990 (**Table 3**). Paired series t-test value ranges respectively from 7.3 to 7.7. In comparison using 10-year moving averages, correlation rises to 0.79 for model A and 0.85 for model B (**Table 3**, **Figure 3**).

4. Discussion

A 16-series multiproxy as well as a 12-series tree-growth based record produced feasible reconstruction models for the AMO. These networks of nearly millennial series likely double the length of the existing 450-year proxy AMO back to the 11th century. Both of the new models are statistically highly significant, indicating strong linear (statistical) relationships. Although the 16-series multiproxy is superior in model performance (measured as r^2), both of our two models generally work at least as well as the one by Gray *et al.* [10]. According to these authors [10] the correlation between their reconstruction and the annual observed AMO is 0.64 without filtering and 0.84 after filtering. In addition, the new models are nearly independent from the old model. They have only one partly common component series, *i.e.* some data shared by the previous and updated versions of the Torneträsk tree-ring chronology from northern Sweden.

Gray *et al.* [10] reported that the output from their model has RE = 0.25 (LC_EV). Our models A and B with RE = 0.37 and 0.21 respectively compare well with this. Only the LC_EV verification was applied by Gray *et al.* [10]. We have now enhanced the procedure using two split periods for cross-validation in addition to applying the more searching CE statistic (not used previously in AMO-reconstructions). Both periods here perform well allowing feasible independent verification.

The two calibration and verification periods show that the AMO switch between negative and positive shifts (warm and cool phases) in 1920s do not alter the time stability of these equations (*i.e.* similar calibration and verification statistics in EC_LV and LC_EV). RE and CE are central tools in dendroclimatology assessing the

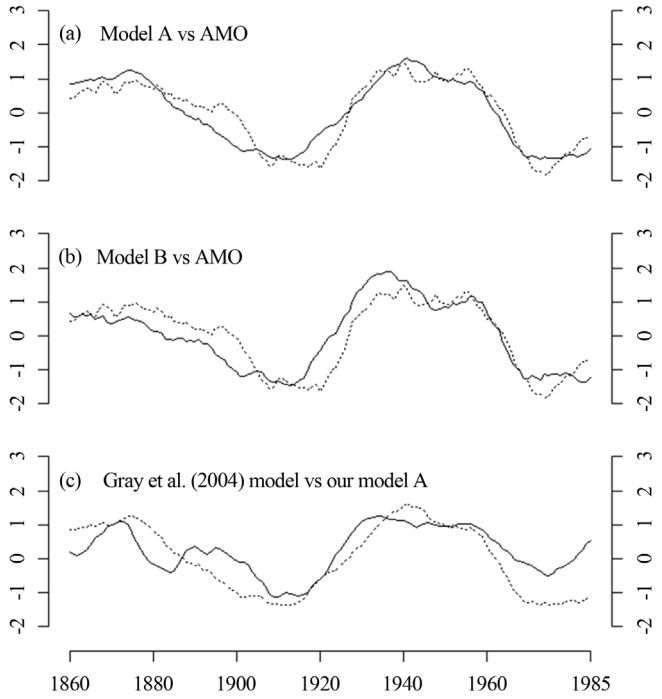

Figure 3. 10-year moving averages (1860-1985) of actual (dotted line) and estimated values: the 16 series multiproxy (a), 12 series tree-growth based proxy (b) and in (c) model A series (dotted) vs the one built by Gray *et al.* [10].

Table 3. Correlation and Students t-statistic between the AMO and our models A, B and the reconstruction by Gray *et al.* [10] during 1856-1990 using both filtered and unfiltered values. The latter is also compared with the new models A and B.

	r	t-value
Model A vs AMO		
Unfiltered	0.67	10.45
Filtered	0.92	25.64
Model B vs AMO		
Unfiltered	0.60	8.55
Filtered	0.87	19.29
The model by Gray *et al.* vs our model A		
Unfiltered	0.53	7.3
Filtered	0.79	14.34
The model by Gray *et al.* vs our model B		
Unfiltered	0.54	7.7
Filtered	0.85	17.71

general feasibility of a model, with zero indicating that the reconstruction model performs no better as a predictor than the mean value of the calibration (RE) or verification (CE) period. The late calibrations of both models A and B are slightly better than the early ones. The multidecadal scale is enhanced using 10-year running means, which effectively removes any high frequency characteristics in the data. Correlation of especially filtered series—AMO vs our models A and B—compares very favourably with the new models.

The geographical distribution of these data indicate that an AMO-like oscillation is more widely spread over

the Northern Hemisphere than was evident in the previous more basin-wide data of Gray *et al.* [10], the focus of which was closer to the North Atlantic rim. The improved statistics of the new models further support the idea that a strong multidecadal scale variability (with a reasonable match with the AMO) is not limited to regions bordering the North Atlantic. In addition the AMO-signal evidently does not weaken from the Atlantic towards the outer fringes of this network. In the past the AMO index has been linked to various proxy temperatures and rainfall over much of the Northern Hemisphere as well as to a wide range of other climate parameters. Similar periodicity has been found in e.g. Atlantic Arctic sea ice [21], winter temperatures in Europe, African drought frequency [21] [22], Asian summer monsoons [23] [24] and climate parameters from Northeastern Asia [24] as well as South American rainfall [25].

Some other types of studies with denser networks give support to the possibility of an AMO signature on global multidecadal climate variability [7] [24] [26]. Although part of the speleothem and sediment data in our analyses come from maritime regions, the majority of proxy series originate from terrestrial (continental) regions. Thus according to these data the multidecadal climatic signal is persistent in the proxy network from the bulk of the Northern Hemisphere. This confirms previous studies showing AMO-links from far-away regions [5] [21] [22] [24]-[26]. For example Arctic air temperature and pressure have been shown to display strong multi-decadal variability on similar time scales [27]. According to Schlesinger and Ramankutty [1] the surface temperature records for 11 geographical regions shows that a 65 - 70-year oscillation is the statistical result of 50 - 88-year oscillations for the North Atlantic Ocean and it's bounding Northern Hemisphere continents. In addition, also Delworth and Mann [6] extracted a multidecadal signal from global surface-temperature reconstructions.

5. Conclusions

This paper was devoted to the calibration of proxies against the AMO, *i.e.* extracting an AMO signal. The two networks of proxy data provided new and well replicated transfer models for the AMO. Despite using nearly millennium-long records, the models perform very well, in particular the multiproxy option. In addition, both models now easily passed vigorous cross-calibration-verification tests. We used split periods and also the CE statistic, *i.e.* comparison of reconstruction also to the mean of verification period and not just to that of the calibration period as in previous studies.

These proxies will help to extend the current AMO record backwards in time from AD 1567 to exceed 900 years in record length. Work continues on analyses of the actual long-term proxy reconstruction in various frequency ranges during the past centuries. Such a long time-series is needed in future comparisons of the 20th century modes of variability to those of the past as well as to higher frequency atmospheric modes, e.g. North Atlantic Oscillation and Arctic Oscillation.

Somewhat surprisingly the new networks showed a meaningful response to the AMO in a more extensive spatial distribution of the phenomenon in proxies than the previous model of Gray *et al.* [10]. Generally the two tree-growth-based models—old model of Gray *et al.* [10] and our new model B are obviously somewhat more alike than the new multiproxy model A, which however has the best fit to the observed AMO in both annual and decadal scales.

References

[1] Schlesinger, M.E. and Ramankutty, N. (1994) An Oscillation in the Global Climate System of Period 65-70 Years. *Nature*, **367**, 723-726. http://dx.doi.org/10.1038/367723a0

[2] Kerr, R.A. (2005) Atlantic Climate Pacemaker for Millennia Past, Decades Hence? *Science*, **309**, 41-43. http://dx.doi.org/10.1126/science.309.5731.41

[3] Parker, D. (2007) Decadal to Multidecadal Variability and the Climate Change Background. *Journal of Geophysical Ressearch*, **112**, Article ID: D18115.

[4] Enfield, D.B., Mestas-Nuñes, A.M. and Trimble, P.J. (2001) The Atlantic Multidecadal Oscillation and Its Relation to Rainfall and River Flows in the Continental U.S. *Geophysical Research Letters*, **28**, 2077-2080. http://dx.doi.org/10.1029/2000GL012745

[5] Dong, B., Sutton, R.T. and Scaife, A.A. (2006) Multidecadal Modulation of El Niño—Southern Oscillation (ENSO) Variance by Atlantic Ocean Sea Surface Temperatures. *Geophysical Research Letters*, **33**, Article ID: L08705. http://dx.doi.org/10.1029/2006GL025766

[6] Delwoth, T.L. and Mann, M.E. (2000) Observed and Simulated Multidecadal Variability in the Northern Hemisphere.

Climate Dynamics, **16**, 661-676. http://dx.doi.org/10.1007/s003820000075

[7] Mann, M.E., Zhang, Z., Rutherford, S., Bradley, R.S., Hughes, M.K., Shindell, D., Ammann, C., Faluvegi, G. and Fenbiao, N. (2009) Global Signatures and Dynamical Origins of the Little Ice Age and Medieval Climate Anomaly. *Science*, **326**, 1256-1260. http://dx.doi.org/10.1126/science.1177303

[8] Knudsen, M.F., Jacobsen, B.H., Seidenkrantz, M.-S. and Olsen, J. (2014) Evidence for External Forcing of the Atlantic Multidecadal Oscillation Since Termination of the Little Ice Age. *Nature Communications*, **5**, Article ID: 3323.

[9] Otterå, O.H., Bentsen, M., Drange, H. and Suo, L. (2010) External Forcing as a Metronome for Atlantic Multidecadal Variability. *Nature Geosciences*, **3**, 688-694. http://dx.doi.org/10.1038/ngeo955

[10] Gray, S.T., Graumlich, L.J., Betancourt, J.L. and Pederson, G.T. (2004) A Tree-Ring Based Reconstruction of the Atlantic Multidecadal Oscillation Since 1567 AD. *Geophysical Research Letters*, **31**, Article ID: LI2205. http://dx.doi.org/10.1029/2004GL019932

[11] Fritts, H.C. (1976) Tree Rings and Climate. Academic Press, New York.

[12] Cook, E.R., Buckley, R.D., D'Arrigo, R.D. and Peterson, M.J. (2002) Warm-Season Temperatures since 1600 BC Reconstructed from Tasmanian Tree Rings and Their Relationship to Large-Scale Sea Surface Temperature Anomalies. *Climate Dynamics*, **16**, 79-91. http://dx.doi.org/10.1007/s003820050006

[13] Cook, E.R. and Peters, K. (1981) The Smoothing Spline: A New Approach to Standardizing Forest Interior Tree-Ring Series for Dendroclimatic Studies. *Tree-Ring Bulletin*, **41**, 45-53.

[14] Lindholm, M., Aalto, T., Grudd, H., McCarroll, D., Ogurtsov, M. and Jalkanen, R. (2012) Common Temperature Signal in Four Well-Replicated Tree Growth Series from Northern Fennoiscandia. *Journal of Quaternary Science*, **27**, 828-834. http://dx.doi.org/10.1002/jqs.2575

[15] Lindholm, M., Ogurtsov, M., Jalkanen, R., Grudd, H., Gunnarson, B.E. and Aalto, T. (2014) Six Temperature Proxies of Scots Pine from the Interior of Northern Fennoscandia Combined in Three Frequency Ranges. *Journal of Climatology*, **2014**, Article ID: 578761. http://dx.doi.org/10.1155/2014/578761

[16] Kaplan, A., Cane, A. and Kushnir, Y. (1998) Analysis of Global Sea Surface Temperatures 1856-1991. *Journal of Geophysical Research*, **103**, 18575-18589. http://dx.doi.org/10.1029/97JC01736

[17] Briffa, K.R., Jones, P.D., Pilcher, J.C. and Hughes, M. (1988) Reconstructing Summer Temperatures in Northern Fennoscandia Back to AD 1700 Using Tree-Ring Data from Scots Pine. *Arctic and Alpine Research*, **20**, 385-394. http://dx.doi.org/10.2307/1551336

[18] Cook, E.R., Briffa, K.R. and Jones, P.D. (1994) Spatial Regression Methods in Dendroclimatology: A Review and Comparison of Two Techniques. *International Journal of Climatology*, **14**, 379-402. http://dx.doi.org/10.1002/joc.3370140404

[19] Guiot, J. (1990) Methods of Calibration. In: Cook, E.R. and Kairiukstis, L.A., Ed., *Methods of Dendrochronology*: *Applications in the Environmental Science*, Kluwer Academic Publishers, Dordrect, 165-178.

[20] National Research Council (2006) Surface Temperature Reconstruction for the Last 20,000 Years. National Academies Press, Washington DC.

[21] Miles, M.W., Divine, D.V., Furevik, T., Jansen, E., Moros, M. and Ogilvie, A.E. (2014) A Signal of Persistent Atlantic Multidecadal Variability in Arctic Sea Ice. *Geophysical Research Letters*, **41**, 463-469. http://dx.doi.org/10.1002/2013GL058084

[22] Folland, C.K., Palmer, T.N. and Parker, D.E. (1986) Sahel Rainfall and Worldwide Sea Temperatures. *Nature*, **320**, 602-606. http://dx.doi.org/10.1038/320602a0

[23] Lu, R., Dong, B. and Ding, H. (2006) Impact of the Atlantic Multidecadal Oscillation on the Asian Summer Monsoon. *Geophysical Research Letters*, **33**, Article ID: L24701. http://dx.doi.org/10.1029/2006GL027655

[24] Wang, Y., Li, S. and Luo, D. (2009) Seasonal Response of Asian Monsoonal Climate to the Atlantic Multidecadal Oscillation. *Journal of Geophysical Research*, **114**, Article ID: D02112. http://dx.doi.org/10.1029/2008JD010929

[25] Kayano, M.T. and Capistrano, V.B. (2014) How the Atlantic Multidecadal Oscillation (AMO) Modifies the ENSO Influence on the South American Rainfall. *International Journal of Climatology*, **34**, 162-178. http://dx.doi.org/10.1002/joc.3674

[26] Wang, X., Brown, P.M., Zhang, Y. and Song, L. (2011) Imprint of the Atlantic Multidecadal Oscillation on Tree-Ring Widths in Northeastern Asia Since 1568. *PLoS ONE*, **6**, e22740. http://dx.doi.org/10.1371/journal.pone.0022740

[27] Polyakov, I.V., Alekseev, G.V., Bekryaev, R.V., Bhatt, U., Colony, R.L., Johnson, M.A., Karklin, V.P., Makshtash, A.P., Walsh, D. and Yulin, A.V. (2002) Observationally Based Assessment of Polar Amplification of Global Warming. *Geophysical Research Letters*, **29**, 1878. http://dx.doi.org/10.1029/2001GL011111